Tantalum doping in HfO_2: Orthorhombic phase formation at ambient conditions and change in path of pressure induced structural evolution

S. Pathak,[1,2] P. Das,[1,2,a)] M. Sahu,[2,3] K. L. Pande,[3] G. Mandal,[4] and G. R. Patkare[5]
[1)] *Experimental Nuclear Physics Division, Variable Energy Cyclotron Centre, Kolkata 700064, India*
[2)] *Homi Bhabha National Institute, Anushaktinagar, Mumbai 400094, India*
[3)] *Radioanalytical Chemistry Division, Bhabha Atomic Research Centre, Mumbai 400085, India*
[4)] *Centre for Rural and Cryogenic Technologies, Jadavpur University, Kolkata 700032, India*
[5)] *Technical Physics Division, Bhabha Atomic Research Centre, Mumbai 400085, India*

(Dated: 17 February 2022)

A systematic study of orthorhombic phase formation at ambient conditions beyond a critical concentration of dopant Tantalum (Ta) in HfO_2 is reported. The effect on the path of structural evolution due to Ta doping in HfO_2 was also investigated. Studies on Ta doped HfO_2 samples and their path of structural evolution under compression has significant implications for materials undergoing β-decay. The effect of continual doping due to β-decay from geophysical point of view is discussed.

It is well known that HfO_2 exhibits polymorphism under high pressure and temperature and it has remained a topic of interest for the application potential in different fields[1,2]. Experimental studies reveal that HfO_2 has baddeleytile structure with monoclinic symmetry ($P2_1/c$) at ambient conditions. Transformation to orthorhombic-I, orthorhombic-II and tetragonal structural phases occur sequentially under high pressure conditions[3,4]. As there exists disagreement regarding phase boundaries and their space groups, experimental and theoretical endeavors continues till date for understanding the properties of HfO_2. *In situ* X-ray diffraction experimental studies of HfO_2 by Adams et al.[5] mentioned that the phase transformation from initial monoclinic phase begins at 2.6 GPa and the diffraction peaks could be indexed on an orthorhombic cell (*Pbcm*, Z=4) for the new phase. Though Jayaraman et al.[3] and Arashi[6] from their Raman scattering studies on a single crystal specimen observed that phase transformation occuring at a higher pressure of 4.3 ± 0.3 GPa, they were in agreement regarding orthorhombic-I phase belonging to the space group, *Pbcm* with Adams et al.[5]. Kourouklis et at.[7] did not observe pressure-induced phase transformation upto 12 GPa in their Raman scattering experiment with HfO_2, apparently due to poor optical quality of their investigated powder sample[6]. On the other side, Legar et al.[4] observed the transformation at higher pressure, around 10 GPa and indicated the orthorhombic-I phase to be *Pbca*. Ohtaka et al.[8,9] reported the space group as *Pbca* for orthorhombic-I phase of HfO_2 sample synthesized at high temperature and pressure. Several experimental studies have been carried out with HfO_2 samples quenched from higher temperature and pressure[10–14], where the sample exists far from thermodynamical equilibrium and cotunnite structure has been reported as the high pressure orthorhombic-II phase. But pressure induced *in situ* experiments with HfO_2 have not shown any signature of cotunnite structure as the orthorhombic-II phase[3,4]. We may conclude from these reports that there is uncertainty regarding initiation of orthorhombic-I phase as a high pressure phase of HfO_2 and possibly depends on sample preparation or impurity present in the samples. Moreover the ambient monoclinic phase of HfO_2 coexist in pressure range where orthorhombic-I phase has been observed, so unambiguous determination of space group of orthorhombic-I has been difficult.

Following reports on HfO_2 systems exhibiting ferroelectric properties[15] interest in orthorhombic phase of HfO_2 renewed. Extensive studies continued in search of ferroelectricity with different dopants e.g., Si[16–19], Al[20], Y[21], Gd[22], La[23,24], Sr[25] in HfO_2. First principle calculations indicated low free energies and spontaneous electric polarization for two orthorhombic polar phases (space groups $Pca2_1$ and $Pmn2_1$) and thus are considered as the most viable ferroelectric phases of hafnia[26]. Investigation on Si-doped HfO_2 (Si:HfO2) powders with 3, 5, or 9 at.% doping showed minimal impact of doping on lattice parameters[27]. Applied pressure in these samples induced monoclinic to orthorhombic phase transition at a relatively higher pressure in the range of 7 to 15 GPa compared to undoped samples. However, space group of the orthorhombic phase was not reported.

A recent study on HfO_2 using time differential perturbed angular correlation (TDPAC) technique[28] reported observation of orthorhombic phase in HfO_2 at ambient condition. This invoked the possibility that Tantalum could be the inducing agent for the orthorhombic phase. In TDPAC experiments, radioactive ^{181}Hf isotope, the probe nuclei are introduced in the sample by irradiation or through chemical route. The probe ^{181}Hf undergoes nuclear β^--decay leading to formation of

[a)] Electronic mail: parnika@vecc.gov.in.

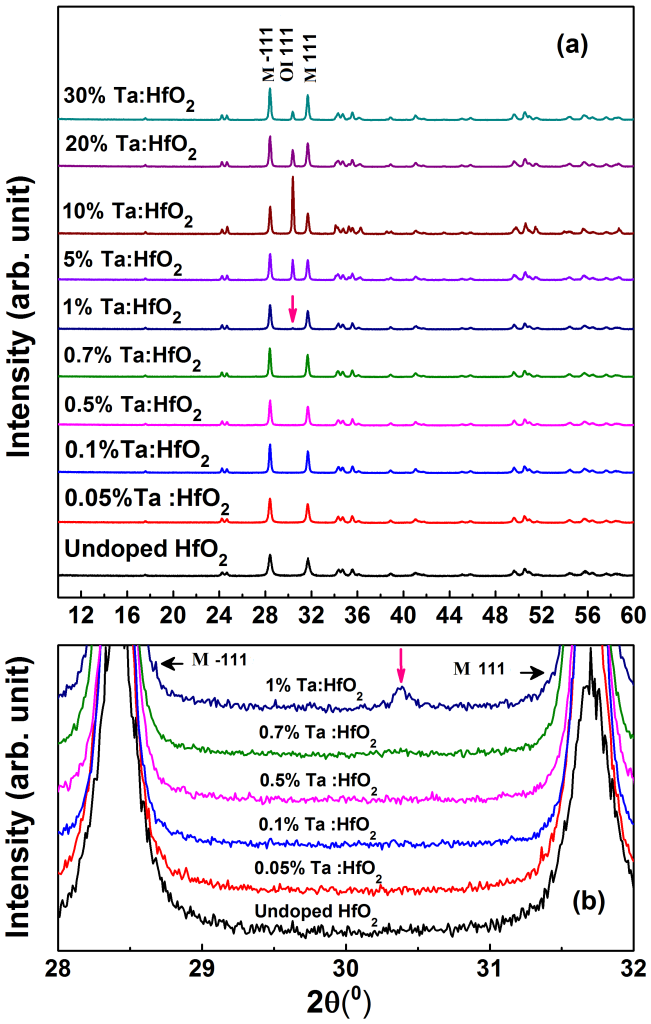

FIG. 1. (a) XRD patterns of undoped and Ta-doped HfO_2 in lab Cu-$K_{\alpha 1}$ X-ray source and (b) enlarged figure. A new peak with low relative intensity between most intense -111 and 111 monoclinic peaks for minimum 1% Ta doping in HfO_2 is marked with arrow and it is signature of orthorhombic-I phase formation.

daughter ^{181}Ta in an excited state. In the de-excitation process through gamma emission, there is emission of two gamma photons 133-482 keV in cascade with an intermediate state with life time of 10.8 ns[29]. This characteristic property of cascade gamma emission with a suitable intermediate state life-time makes ^{181}Hf $\rightarrow$ ^{181}Ta suitable as a TDPAC probe. Hyperfine interaction of the ^{181}Ta nucleus at this intermediate $5/2^+$ state of the gamma cascade with electron field gradient (EFG) of HfO_2 at the decaying nucleus gives information about the electronic environment around the probe nuclei. Thus any sample studied using ^{181}Hf as TDPAC probe gets naturally doped with Ta following ^{181}Hf$\rightarrow$^{181}Ta β^--decay. So, HfO_2 sample studied by TDPAC technique also contains ^{181}Hf probe and eventually gets doped with Ta. It is well known that doping can induce phase transformation and a few examples of systems exhibiting such transformation are listed here[30–33]. The possibility of phase transformation due to Ta doping in HfO_2 is explored in this work.

Ta-doped samples with 0.05%, 0.1%, 0.5%, 0.7%, 1%, 5%, 10%, 20% and 30% doped (mol%) HfO_2 were synthesized by solid state reaction route using precursors such as HfO_2 and Ta_2O_5. The required quantity of reactants were grinded, mixed and pelletised. The pellets were heated stepwise at various temperatures of 1200^0C, 1300^0C and 1400^0C for $\sim$ 20 hours each and soaked for 12 hours at each temperature. Before heating at next higher temperature, the process of grinding, mixing and pelletisation was repeated. Energy dispersive X-ray spectroscopy (EDS) analysis shows $\sim$ 7% of Zr-impurity in the doped samples.

TABLE I. Volume of monoclinic cell and proportion of orthorhombic-I phase formation in HfO_2 with different concentration of Ta doping determined from Cu-$K_{\alpha 1}$ XRD experiment

Concentration of Ta doping	Monoclinic Cell volume ($\AA^3$)	Orthorhombic-I phase percentage[a]
1%	138.039(6)	1%
5%	138.454(12)	23%
10%	138.911(19)	47%
20%	139.707(28)	19%
30%	140.625(21)	9%

[a] Estimated error in the phase percentage values are $\sim$ 3%

Laboratory XRD experiment at ambient condition using Cu-$K_{\alpha 1}$ source was performed at BARC, Mumbai. The measurements were performed with Bragg-Brentano geometry using Rigaku Smart Lab diffractometer and diffracted rays were detected by D/teX Ultra 250 1D silicon strip X-ray detector[34]. The diffraction patterns for undoped and the doped samples are shown in Fig. 1(a). In the enlarged figure [Fig. 1(b)] appearance of a new peak between the most intense monoclinic -111 and 111 peaks for 1% doped HfO_2 sample is clearly observed. With increasing Ta doping concentration to 5% and 10% the relative intensity of this peak, identified as signature orthorhombic-I 111 peak of HfO_2[5,35], increased indicating enhancement of orthorhombic-I phase formation in the samples. 10% Ta doping showed maximum transformation, $\sim$ 50%. However, as the doping concentration increased to 20% and 30%, relative intensity of the orthorhombic-I peak decreased as shown in Fig. 1(a). The unit cell volume determined from X-ray diffraction data of HfO_2 with increasing Ta-doping concentration remains nearly same up to 1% doping and increases by very small proportion beyond it [Table I] indicating that there is not much distortion in the crystal structure of HfO_2. Thus orthorhombic-I polymorph is formed by Ta doping in ambient conditions co-existing with the monoclinic phase and formation of this orthorhombic-I phase

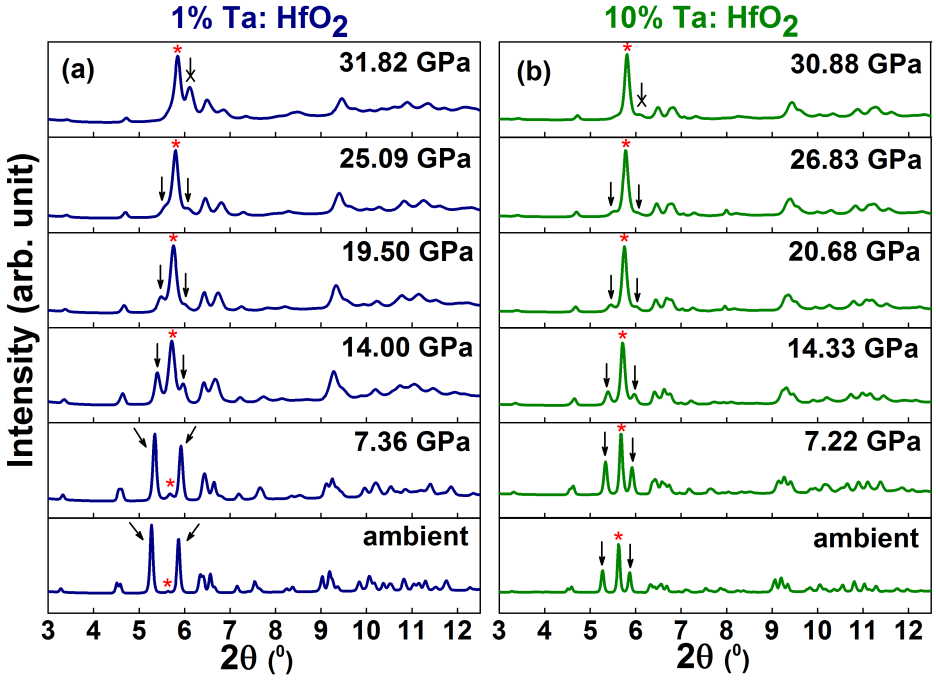

FIG. 2. Synchrotron XRD patterns of (a) 1% Ta:HfO_2 and (b) 10% Ta:HfO_2. Asterisk shows the most intense 111 peak of orthorhombic-I phase. Arrows indicate principle -111 and 111 peaks of monoclinic phase and the crossed arrows depict appearing 111 peak from tetragonal phase at the highest pressures.

depends on the concentration of the dopant Ta in HfO_2 .

An orthorhombic-I polymorph formation similar to the high pressure phase of undoped HfO_2 invoked an interest for a study on these newly formed materials (Ta:HfO_2) under compression. Angle Dispersive X-ray Powder Diffraction (ADXRPD) experiment was performed at Extreme Condition Beamline (ECB)[36] in the brilliant synchrotron facility of PETRA-III (spectral brightness $> 10^{21}$ photons/(s mm^2 mrad^2 0.1% bw)). Monochromatic (42.7 keV; $\Delta E/E \sim 2\times10^4$) and highly focussed (divergence: 0.26 mrad $\times$ 0.25 mrad) beam with minute beam size ($\sim$ 8(V) μm $\times$ 3.2(H) μm) was produced at the sample position. Symmetric diamond anvil cell (DAC) with 300 μm anvil size was used in the experiment. $\sim$ 60 μm diameter hole was laser drilled inside Rhenium (Re) gasket and fixed on the diamond anvil with glue. Sample was loaded in the hole along with silicone oil and ruby grains which acts as pressure transmitting medium and pressure calibrant respectively. Pressure was applied using a gas membrane after locking the DAC. Pressure gradient appears in silicone oil at 3 GPa and its rapid increase beyond 12 GPa, probably due to a phase transition[37] makes the system environment quasi-hydrostatic. Fast area scintillator (CsI) detector XRD 1621 (Perkin-Elmer) detected the diffracted beam. The experiment was performed in axial geometry, i.e., the beam was passing through the diamond in the parallel direction of its load axis. The sample to detector geometry was calibrated with powder X-ray diffraction (XRD) of standard CeO_2 (NIST) and the 2D diffraction images were integrated to I-2θ patterns using Dioptas program[38].

Structural evolution of 1% and 10% Ta-doped HfO_2 samples were studied under quasi hydrostatic condition upto $\sim$ 32 GPa pressure in this experimental set up and the XRD patterns are shown in Fig. 2. The relative intensity of the major 111 peak of orthorhombic-I phase increases with pressure indicating increased conversion to the orthorhombic-I phase and diminution of the monoclinic phase occurs simultaneously. Around 30 GPa, the monoclinic phase diminishes and a new peak appears for both 1% and 10% Ta:HfO_2 samples at $\sim 2\theta = 6.1^0$, recognised as 111 diffraction peak of high pressure tetragonal phase of HfO_2. So a phase transition occurs from orthorhombic-I to tetragonal structure around 30 GPa confirming the stability of orthorhombic-I phase in the pressure range starting from ambient conditions. It is to be noted that no signature indicating the orthorhombic-II phase formation has been observed in the Ta-doped samples under pressure.

Rietveld refinement of the XRD patterns at ambient and high pressures were performed using General Structure Analysis System GSAS[39]. Very low texture coefficients (J) found from Rietveld refinement indicate absence of preferred orientation in the samples. Refinement of the synchrotron XRD pattern for 1% Ta-doped HfO_2 is shown in Fig. 3 having reduced χ^2= 1.06. Definitive determination of space group was not possible from this XRD analysis, but a better fitting parameter indicated *Pbcm* symmetry for the orthorhombic-I phase. Though proportion of orthorhombic-I phase for 10% Ta-doped

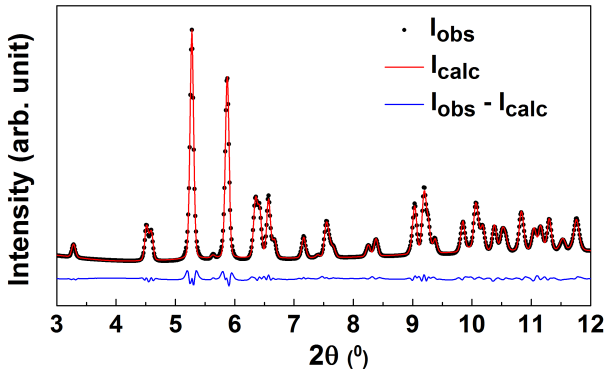

FIG. 3. Rietveld refinement of synchrotron XRD pattern for 1% Ta:HfO_2 at ambient condition. Line below the fitting pattern shows difference between observed and fitted intensity.

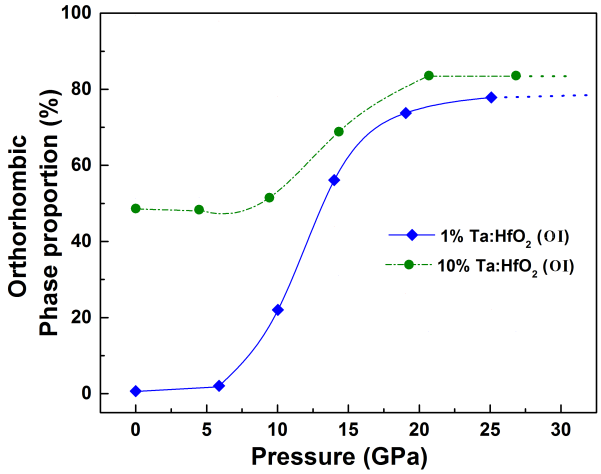

FIG. 4. Variation of transformed orthorhombic-I (OI) phase proportion with pressure for 1% and 10% Ta:HfO_2. Estimated error in the phase proportion values are $\sim 1\%$. Dot's indicate highest pressures reached in this experiment.

HfO_2 sample ($\sim 50\%$) is comparatively much higher than 1% doped sample ($\sim 0.7\%$) at ambient condition, rate of conversion to orthorhombic-I phase with pressure is much faster for 1% doped sample as shown in Fig. 4. Orthorhombic-I phase reaches to a saturation for both 1% and 10% doped samples ~ 30 GPa pressure.

The study of pressure induced structural evolution gives information regarding bulk modulus. Bulk modulus (B_0) and its derivative (B_0') at ambient condition were evaluated by fitting unit cell volume with pressure for both the monoclinic and orthorhombic-I phases in 1% and 10% Ta:HfO_2 [Fig. 5] with 3rd order Birch-Murnaghan equation[40]. 10% Ta:HfO_2 has higher bulk modulus relative to 1% doping for monoclinic phase whereas the value is similar for both the doping percentages in case of orthorhombic-I phase[Table II]. Bulk moduli of the respective phases observed in doped sample Ta:HfO_2 are higher than reports on undoped HfO_2 existing in monoclinic phase[3,41–45] and high pressure orthorhombic-I phase[4,41–44]. Our preliminary study based on semi-empirical model of hardness (H)[46] indicates that the orthorhombic-I phase formed is harder than the monoclinic phase.

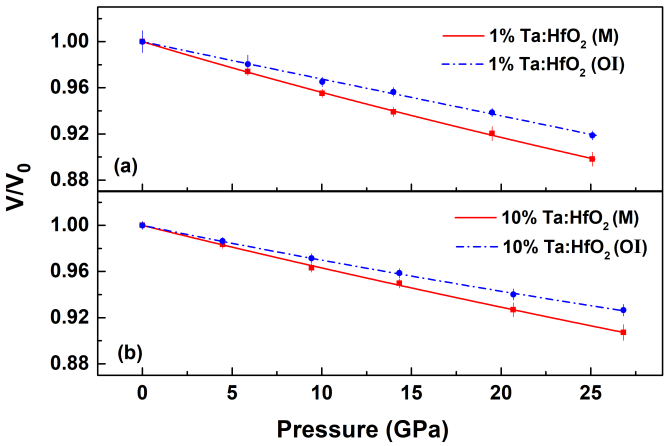

FIG. 5. 3rd order Birch-Murnaghan fitting to volume vs pressure variation for monoclinic (M) and orthorhombic-I (OI) phases for (a) 1 % Ta:HfO_2 and (b) 10% Ta:HfO_2.

TABLE II. Bulk modulus (B_0) and its derivative (B_0') at ambient condition for monoclinic (M) and orthorhombic-I (OI) phases in 1% and 10% Ta-doped HfO_2

	Parameters	M	OI
1% Ta	B_0	213 ± 5	305 ± 14
	B_0'	2.0 ± 0.5	0.0 ± 1.0
10% Ta	B_0	259 ± 9	313 ± 9
	B_0'	1.5 ± 0.5	2.9 ± 1.0

In summary, formation of orthorhombic-I phase of HfO_2 occurs at ambient condition for minimum 1 mol % or higher concentration of Ta doping and this phase formation increases with enhanced Ta doping upto 10 mol %. Further increase in the doping concentration (20% and 30%) results decrease in the orthorhombic-I phase formation. The path of structural phase evolution for Ta-doped HfO_2 under compression is different from undoped HfO_2 as no signature of orthorhombic-II phase is observed in high pressure condition. The orthorhombic-I phase is relatively more stable over a wide pressure range. Understanding the dynamics of phase transformation induced by Ta doping in HfO_2 needs further investigations.

This study has special significance from geophysical point of view considering radioactive decay in the Earth. It is claimed that the heat from radioactive decays contributes about half of Earths total heat flux[47]. Due to radioactive decays the composition of the Earth

would change; particularly in case of β-decay atomic number of the constituents would change by one unit. This study implies that stuctural evolution may take a different path deep inside the Earth where high pressure condition exists. A highly radioactive zone over a span of time would have a different composition and structural evolution is expected to be different compared to the inactive zones.

The authors are thankful to Dr. Ruma Gupta, Fuel Chemistry Division, Bhabha Atomic Research Centre for the EDS measurement. They are grateful to Dr. Anna Pakhomova, DESY, Germany for her support in the experiment at PETRA-III and Dr. Tilak Das, Universit degli Studi di Milano-Bicocca, Italy for useful discussions. The authors thank Dr. G. D. Mukherjee, IISER Kolkata, India for helping them in DAC operation. The authors thank Dept. of Science and Technology, Govt. of India for financial assistance in the experiment at PETRA-III and Mr. Santanu Pathak acknowledges Dept. of Atomic Energy, Govt. of India for his research fellowship.

[1] L. Qi-Jun, Z. Ning-Chao, L. Fu-Sheng, and L. Zheng-Tangi, Chin. Phys. B. **23**, 047101 (2014).
[2] A. P. Huang, Z. C. Yang, and P. K. Chu, in *Advances in Solid State Circuit Technologies*, edited by P. K. Chu (2010) p. 333, intech ed.
[3] A. Jayaraman, S. Wang, and S. Sharma, Phys. Rev. B **48**, 9205 (1993).
[4] J. M. Leger, A. Atouf, P. E. Tomaszewski, and A. S. Pereira, Phys. Rev. B **48**, 93 (1993).
[5] D. M. Adams, S. Leonard, D. R. Russell, and R. J. Cernik, J. Phys. Chem. solids **52**, 1181 (1991).
[6] H. Arashi, J. Am. Ceram. Soc. **75**, 844 (1992).
[7] G. A. Kourouklis and E. Liarokapis, J. Am. Ceram. Soc. **74**, 520 (1991).
[8] O. Ohtaka, T. Yamanaka, and S. Kume, Nippon Seramikkusu Kyokai Gakujutsu Ronbunshi **99**, 826 (1991).
[9] O. Ohtaka, T. Yamanaka, and S. Kume, J. Am. Ceram. Soc. **78**, 233 (1995).
[10] L. Liu, J. Phys. Chem. Solids **41**, 331 (1980).
[11] S. Desgreniers and K. Lagarec, Phys. Rev. B **59**, 8467 (1999).
[12] J. Haines, J. M. Legar, S. Hull, J. P. Petitet, A. S. Pereira, C. A. Perottoni, and J. A. H. da Jornada, J. Am. Ceram. Soc. **80**, 1910 (1997).
[13] R. Suyama, H. Horiuchi, and S. Kume, Yogyo-Kyokai-Shi **95**, 567 (1987).
[14] N. A. Bendeliani, S. V. Popova, and L. P. Vereschagin, Geochem. Int. **4**, 557 (1967).
[15] T. S. Böscke, J. Müller, D. Braühaus, U. Schröder, and U. Böttger, Appl. Phys. Lett. **99**, 102903 (2011).
[16] L. Zhao, M. Nelson, H. Aldridge, C. M. F. T. Iamsasri, J. S. Forrester, T. Nishida, S. Moghaddam, and J. L. Jones, J. App. Phys. **115**, 034104 (2014).
[17] P. D. Lomenzo, Q. Takmeel, C. M. Fancher, C. Zhou, N. G. Rudawski, S. Moghaddam, J. L. Jones, and T. Nishida, IEEE Electron Device Lett. **36**, 766 (2015).
[18] D. Hou, C. M. Fancher, L. Zhao, G. Esteves, and J. L. Jones, J. Appl. Phys. **117**, 244103 (2015).
[19] C. Richter, T. Schenk, M. H. Park, F. A. Tscharntke, E. D. Grimley, J. M. LeBeau, C. Zhou, C. M. Fancher, J. L. Jones, T. Mikolajick, and U. Schroeder, Adv. Electron. Mater. **17**, 1700131 (2017).
[20] S. Müller, J. Müller, A. Singh, S. Riedel, J. Sundqvist, and U. Schröder, Adv. Funct. Mater. **22**, 2412 (2012).
[21] J. Müller, U. Schröder, T. S. Böscke, I. Müller, U. Böttger, L. Wilde, J. Sundqvist, M. Lemberger, P. Kücher, T. Mikolajick, and L. Frey, J. Appl. Phys. **110**, 114113 (2011).
[22] X. Sang, E. D. Grimley, T. Schenk, U. Schroeder, and J. M. LeBeau, App. Phys. Lett. **106**, 162905 (2015).
[23] M. G. Kozodaev, A. G. Chernikova, E. V. Korostylev, M. H. Park, U. Schroeder, C. S. Hwang, and A. M. Markeev, Appl. Phys. Lett. **111**, 132903 (2017).
[24] U. Schroeder, C. Richter, M. H. Park, T. Schenk, M. Pešić, M. Hoffmann, F. P. G. Fengler, D. Pohl, B. Rellinghaus, C. Zhou, C. C. Chung, J. L. Jones, and T. Mikolajick, Inorganic Chemistry **57**, 2752 (2018).
[25] T. Schenk, S. Mueller, U. Schroeder, R. Materlik, A. Kersch, M. Popovici, C. Adelmann, S. V. Elshocht, and T. Mikolajick, in *Proc. Eur. Solid-State Device Res. Conf.*, All ACM Conferences No. 43, p. 260.
[26] T. D. Huan, V. Sharma, J. G. A. Rossetti, and R. Ramprasad, Phys. Rev. B **90**, 064111 (2014).
[27] C. M. Fancher, L. Zhao, M. Nelson, L. Bai, G. Shen, and J. L. Jones, J. Appl. Phys. **117**, 234102 (2015).
[28] D. Banerjee, C. C. Dey, S. W. Raja, R. Sewak, S. V. Thakare, R. Acharya, and P. K. Pujari, in *The Int. Conf. on HYPERFINE Interactions and their Applications*, 43, p. 66.
[29] "Ensdf data of ^{181}ta," https://www.nndc.bnl.gov/ensdf (2005).
[30] Y. Yang, K. Li, and H. Li, Int. J. Appl. Ceram. Technol. **12**, 163 (2015).
[31] P. Wang, R. Zhao, L. Wu, and M. Zhang, RSC Adv. **7**, 35105 (2017).
[32] Y.-R. Zheng, P. Wu, M.-R. Gao, X.-L. Zhang, F.-Y. Gao, H.-X. Ju, R. Wu, Q. Gao, R. You, W.-X. Huang, S.-J. Liu, S.-W. Hu, J. Zhu, Z. Li, and S.-H. Yu, Nature Comm. **9**, 2533 (2018).
[33] S. Kobayashi, Y. Ikuhara, and T. Mizoguchi, Phys. Rev. B **98**, 134114 (2018).
[34] "High-speed 1d silicon strip x-ray detector d/tex ultra 250," Rigaku Journal **30**, 35 (2014).
[35] S. Pathak, G. Mandal, and P. Das, AIP Conf. Proc. **1942**, 030027 (2018).
[36] H.-P. Liermann, Z. Konôpková, W. Morgenroth, K. Glazyrin, J. Bednarčik, E. E. McBride, S. Petitgirard, J. T. Delitz, M. Wendt, Y. Bican, A. Ehnes, I. Schwark, A. Rothkirch, M. Tischer, J. Heuer, H. Schulte-Schrepping, T. Kracht, and H. Franz, J. Synchrotron Rad. **22**, 908 (2015).
[37] S. Klotz, J.-C. Chervin, P. Munsch, and G. L. Marchand, J. Phys. D: Appl. Phys. **42**, 075413 (2009).
[38] C. Prescher and V. B. Prakapenka, High Press. Res. , doi: 10.1080/08957959.2015.1059835 (2015).
[39] A. Larson and R. V. Dreele, Los Alamos National Laboratory Report LAUR **86**, 748 (2000).
[40] F. Birch, Phys. Rev. **71**, 809 (1947).
[41] Y. Al-Khatatbeh, K. K. M. Lee, and B. Kiefer, Phys. Rev. B **82**, 144106 (2010).
[42] J. Kang, E. C. Lee, and K. J. Chang, Phys. Rev. B **68**, 054106 (2003).
[43] J. Zhang, A. R. Oganov, X. Li, K.-H. Xue, Z. Wang, and H. Dong, Phys. Rev. B **92**, 184104 (2015).
[44] J. E. Jaffe, R. A. Bachorz, and M. Gutowsk, Phys. Rev. B **72**, 144107 (2005).
[45] O. L. Anderson, in *Williams Hematology*, edited by E. C. Robertson (McGraw-Hill, New York, 1972) p. 575.
[46] A. Šimůnek, Phys. Rev. B **75**, 172108 (2007).
[47] The KamLAND Collaboration, Nat. Geosci. **4**, 647 (2011).